# Thermal Convection in the Presence of a First-Order Phase Change

Guenter Ahlers, Lars Inge Berge,[a] and David S. Cannell
*Department of Physics and Center for Nonlinear Science, University of California, Santa Barbara, California 93106*
(Received 18 January 1993)

We report experimental results for convection in a thin horizontal layer of a fluid which is heated from below and which undergoes a first-order phase change. For some parameter ranges the denser layer may be stably stratified above the lighter one, as predicted by Busse and Schubert. Over various parameter ranges we observed hexagonal, inverted-hexagonal, and roll flow. Interesting interactions between two-phase convection and Rayleigh-Bénard convection are observed near two codimension-two points.

PACS numbers: 47.20.Bp, 47.27.Te, 47.55.Kf

It is well known that a thin, horizontal layer of quiescent fluid heated from below becomes unstable to convection *via* the Rayleigh-Bénard (RB) mechanism [1], and this system has been used extensively for the study of a great variety of pattern-formation phenomena [2]. It is less widely appreciated that an altogether different instability may occur in such a layer when the fluid undergoes a first-order phase change at a temperature which is intermediate to those of its top and bottom surface. This instability was examined theoretically over two decades ago by Busse and Schubert [3,4], who identified the mechanism and carried out a linear stability analysis. They were motivated by the relevance to geophysical and astrophysical problems. It is believed that phase changes play an important role for convection in the Earth's mantle [5] and in stars, and in geothermal situations where, for instance, water can be stably stratified above steam [4,6]. However, so far as we can determine, there have been virtually no previous laboratory experiments relevant to this interesting problem [7].

Here we report experimental measurements for a liquid-crystal sample with coexisting nematic and isotropic phases in a vertical temperature gradient. For an appropriate range of the top temperature $T_t$ they support the qualitative features predicted by Busse and Schubert. In the experiment, $T_t < T_{NI}$ where $T_{NI}$ is the nematic-isotropic transition temperature. As the heat current $Q$ is increased, the bottom temperature $T_b$ exceeds $T_{NI}$, and soon thereafter, for $\Delta T \equiv T_b - T_t > \Delta T_{c1}$, two-phase convection occurs. For sufficiently large $T_t$, the bifurcation to two-phase convection precedes the bifurcation to RB convection at $\Delta T_c^{RB}$ and thus becomes the primary bifurcation. In that case the pattern which forms first consists of cellular flow arranged in a hexagonal lattice, as is usually the case [2] for a system which lacks reflection symmetry about its horizontal midplane. Upon further increase of $\Delta T$, a pair of secondary bifurcations is encountered at $\Delta T_{c2}$ and $\Delta T_{c3}$. At the first, the hexagonal pattern gives way to rolls. The second yields hexagons once more, but with a flow field which is reversed relative to the original hexagons. Beyond $\Delta T_{c3}$, the flow amplitude can actually decrease with increasing $\Delta T$ until the conduction state is reached again above a critical value $\Delta T_{c4}$. These measurements show the existence of a reentrant conduction state, and dramatically confirm the predicted stability of a heavy fluid layer above a light one in a sufficiently large temperature gradient. The value of $\Delta T_{c4}$ agrees with a theoretical estimate [3] only within a factor of 2 or so; but the theory has been evaluated only for certain idealized parameters which do not pertain quantitatively to our system.

Beyond the reentrant conduction state, the Rayleigh-Bénard instability is encountered for $\Delta T > \Delta T_c^{RB}$. As $T_t$ is reduced, it is possible to change the systems continuously from one in which the reentrant conduction state exists to one in which two-phase convection turns directly and smoothly into Rayleigh-Bénard convection. Interesting pattern interaction between the hexagonal two-phase flow and the roll-like Rayleigh-Bénard flow occurs in the vicinity of the codimension-two point where the two bifurcation lines $\Delta T_{c4}(T_t)$ and $\Delta T_c^{RB}(T_t)$ meet.

The experiment was done with a cylindrical convection cell of thickness $d = 0.404$ cm and radius $R = 20.75d$. The fluid was 4-*n*-pentyl-4'-cyanobiphenyl (5CB), which undergoes a first-order phase transition from an isotropic liquid to a nematic liquid crystal at $T_{NI} = 35.0\,^{\circ}$C. We made measurements in horizontal magnetic fields of strength $H = 42$ G and $H = 1500$ G. At the low field, RB convection occurred in the nematic phase for rather low values of $\Delta T$, thus shifting the codimension-two point at $T^{c1}$ to be reported below to higher temperatures; but otherwise we found no dependence of the bifurcation diagram on $H$ [8]. 5CB has a latent heat [9] $q = 390$ J/mole and a density discontinuity [10] $\Delta\rho/\rho = 0.0024$ with the low-temperature nematic phase more dense. The heat capacity $C_p$ has a singularity, varying from about 480 J/mole K well below $T_{NI}$ to slightly over 600 J/mole K very close to $T_{NI}$ and to 450 J/mole K well above $T_{NI}$ [9,11]. Thus the appropriate scale for temperature differences [3] is $q/C_p \simeq 0.8$ K. The experiments were conducted by holding $T_t$ constant and varying the heat current in steps. Thus the mean temperature, and also the interface position, changed with the current. We made high-resolution heat-transport measurements and had optical access from the top for visualizing the flow patterns. The heat transport will be presented as the Nusselt number $N = \lambda/\lambda_0$, where $\lambda$ is the measured conductivity and $\lambda_0$ is the conductivity of the quiescent fluid.

 

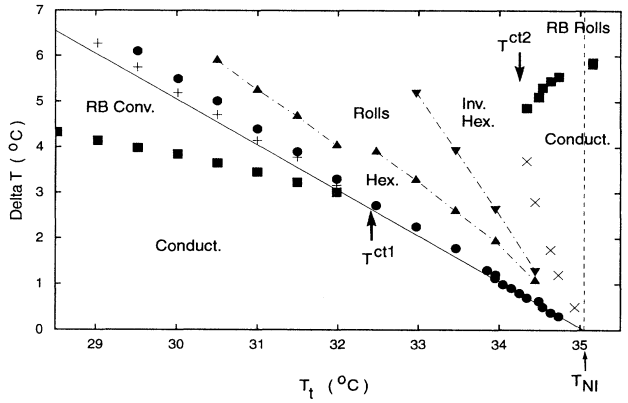


FIG. 1. Critical temperature differences as a function of the top temperature $T_t$. As $\Delta T$ is increased, they mark the following transitions. Squares: Onset of RB convection at $\Delta T_c^{RB}$. Solid line: The bottom of the sample has reached the transition temperature $T_{NI}$; i.e., below it the entire sample is in the nematic phase. Plusses: RB convection becomes visible because isotropic fluid from the sample bottom noticeably affects the director alignment at the top. Circles: Onset of two-phase convection in the form of hexagonal cells at $\Delta T_{c1}$. Upward-pointing triangles connected by dash-dotted lines: Transition to rolls at $\Delta T_{c2}$. Downward-pointing triangles connected by a dash-dotted line: Transition to inverted hexagons at $\Delta T_{c3}$. Crosses: Two-phase convection ceases at $\Delta T_{c4}$. The vertical dashed line corresponds to $T_t = T_{NI}$. The two codimension-two points are indicated by vertical arrows and labeled $T^{ct1}$ and $T^{ct2}$.

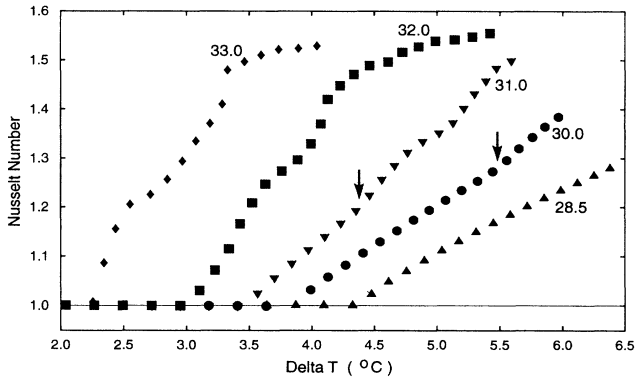


FIG. 2. Nusselt numbers vs $\Delta T$ for the relatively low values of $T_t$ given adjacent to the data sets. For $T_t = 28.5$°C, two-phase convection is never reached (compare with Fig. 1). For $T_t = 30.0$ and 31.0°C, the secondary bifurcation from RB convection to two-phase convection manifests itself by a change in slope of the Nusselt number at the points indicated by the arrows. For $T_t = 33.0$°C, the first bifurcation is directly to two-phase convection.

Although the usual shadowgraph visualization method [12] is not usable for thick liquid-crystal layers since they are not transparent, even very weak flow manifested itself in a variation of the diffuse scattering of ambient light by the elongated molecules which were aligned horizontally at the upper surface [Figs. 3(a) and 3(b)]. Stronger flows caused isotropic fluid to virtually reach the top of the sample and led to black spots or bands corresponding to the flow pattern (all other images in Figs. 3 and 5).

In Fig. 1 we show the critical temperature differences for the various bifurcations encountered as the heat current $Q$ is varied. For $T_t < T^{ct1} \simeq 32.4$°C, the system first becomes unstable to RB convection at $\Delta T = \Delta T_c^{RB}$. This is shown by the left set of solid squares, and occurs before $T_b$ reaches $T_{NI}$. In this case, no pattern was discernible for $\Delta T$ slightly above $\Delta T_c^{RB}$ because the convection rolls have their axes aligned parallel to **H** and the director [13] and do not distort the director field. However, the bifurcation is clearly seen in the Nusselt number, as shown in Fig. 2 by the data for $T_t = 28.5$, 30.0, and 31.0°C. When $\Delta T$ exceeds $T_{NI} - T_t$ (i.e., when $T_b$ exceeds $T_{NI}$), the pattern becomes visible because flow of the isotropic phase at the sample bottom produces a detectable director distortion near the upper sample surface. The corresponding values of $\Delta T$ are shown as plusses in Fig. 1. The solid line in the figure corresponds to $\Delta T = T_{NI} - T_t$, and as expected is only very slightly below the plusses. A typical image is shown in Fig. 3(a). It corresponds to $T_t = 30.0$°C and $\Delta T = 5.445$°C. In all images to be shown, **H** is from left to right, and thus the roll axes in Fig. 3(a) are aligned with **H** [13]. The wave vector in units of $1/d$ is 3.03, which agrees well with the theoretical value [13] 3.10.

For $T_t < T^{ct1}$, further increase of $\Delta T$, and thus of the thickness of the isotropic layer at the bottom of the sample, leads to a secondary bifurcation at $\Delta T_{c1}$. It is shown in Fig. 1 by the solid circles. As can be seen from Fig. 2

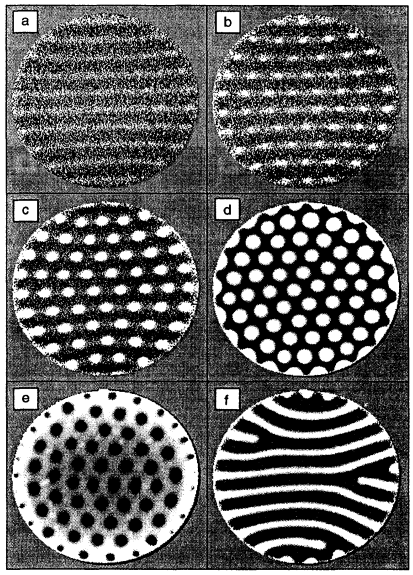


FIG. 3. Images of convection patterns. The magnetic field points from left to right. The values of $T_t$ and of $\Delta T$, in °C, are (a) 30.0 and 5.445, (b) 30.0 and 5.554, (c) 31.0 and 4.885, (d) 34.5 and 0.974, (e) 34.0 and 2.913, and (f) 31.0 and 5.592.

for $T_t = 30.0$ and 31.0°C, it produces a change in the slope of the Nusselt number at the points indicated by the arrows (the run at 28.5°C never reached $\Delta T_{c1}$). More dramatically, it yields a different flow pattern which consists of cellular flow arranged on a hexagonal lattice. Examples are shown in Figs. 3(b) and 3(c). Figure 3(b) is for $T_t = 30.0$°C and $\Delta T = 5.554$°C, and Fig. 3(c) is for $T_t = 31.0$°C and $\Delta T = 4.885$°C. The patterns in Figs. 3(b) and 3(c) are still evolving slightly. After quite long transients they form nearly perfect hexagons. This is shown in Fig. 3(d) for $T_t = 34.5$, but for $\Delta T = 0.974$°C which is still in the region of hexagonal flow (see Fig. 1). This pattern had been equilibrated for about 10 h. Note that the cellular two-phase flow in Figs. 3(b) and 3(c) is aligned with the RB roll flow.

When $T_t$ is increased sufficiently so that $T_b$ exceeds $T_{NI}$ well before $\Delta T_c^{RB}$ is reached, the secondary bifurcation at $\Delta T_{c1}$ becomes the primary one, as seen in Fig. 1. The conduction state now becomes unstable, presumably *via* the two-phase mechanism of Busse and Schubert. Note that $T_t + \Delta T_{c1}$ exceeds $T_{NI}$, thus indicating that a thin layer of the isotropic fluid *below* the *denser* nematic layer is a stable state without convection. The pattern just above $\Delta T_{c1}$ in this case does not differ very much from those shown in Figs. 3(b) and 3(c), as illustrated by the one shown in Fig. 3(d). However, as $\Delta T$ is increased further, a pair of secondary bifurcations, shown as up- and down-pointing triangles connected by dash-dotted lines in Fig. 1, occurs at $\Delta T_{c2}$ and $\Delta T_{c3}$ and leads to a different pattern. The cells [which appeared as bright dots in Figs. 3(b)–3(d)] now show as dark dots as illustrated in Fig. 3(e). This particular image is for $T_t = 34.0$°C and $\Delta T = 2.913$°C. We refer to the two cases as hexagons and inverted hexagons, respectively. We presume that they differ by a reversal of the flow field within the cells, but have no direct velocity measurements. Between the two secondary bifurcations at $\Delta T_{c2}$ and $\Delta T_{c3}$ there is a range over which striped patterns are stable, and we interpret these as corresponding to roll-like convection. As can be seen from the up-pointing triangles in Fig. 1, these rolls also form for $T_t < T^{ct1}$ where two-phase convection sets in as a secondary bifurcation. An example for $T_t = 31.0$°C and $\Delta T = 5.592$°C is shown in Fig. 3(f). The dash-dotted lines drawn through the up-pointing triangles suggest a discontinuity in $\Delta T_{c2}$ near the codimension-two point at $T^{ct1}$. An example of rolls for a larger $T_t$ will be given below in Fig. 5(b).

Although the transition from hexagons to rolls and then to inverted hexagons is a nonlinear problem which has not been investigated theoretically, it can be understood qualitatively in terms of the appropriate amplitude equation [2]. Schematically, this equation has the form $\partial A/\partial t = \epsilon A + g_2 A^2 - g_3 A^3$, where $\epsilon = \Delta T/\Delta T_c - 1$ and where $A$ is the amplitude of the flow field. It is well known [2] that the pattern-stability problem is controlled by the coefficient $g_2$. For a given positive $\epsilon$, hexagons (inverted hexagons) will be stable for a sufficiently large positive (negative) $g_2$. For $g_2$ sufficiently close to zero, rolls will be stable. We conclude from the experimental evidence that $g_2$ depends upon $\Delta T$ for our experimental protocol which held $T_t$ fixed and thus led to an interface position which depended upon $\Delta T$. For an interface position close to the middle of the sample, $g_2$ apparently passes through zero.

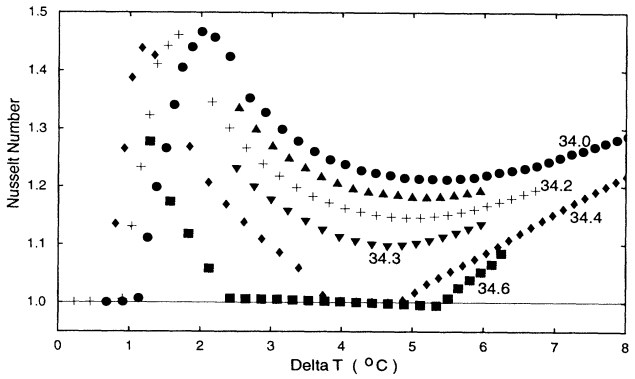


FIG. 4. Nusselt numbers vs $\Delta t$ for the relatively high values of $T_t$ given adjacent to the data sets.

An interesting aspect of the secondary bifurcations is reflected in the Nusselt numbers, as shown in Fig. 4. The heat transport first rises in the region of hexagons. In the inverted-hexagon range it decreases again. For $T_t$ near 34.0°C, $N$ increases once more when $\Delta T$ becomes sufficiently large so that RB convection is expected. The pattern remains essentially unchanged, and is similar to that in Fig. 3(e). An example for $T_t = 34.0$°C and $\Delta T = 5.281$°C is shown in Fig. 5(a). An interesting new feature is the light bridges connecting some of the neighboring cells, but we do not know its significance.

When $T_t$ is increased further, say, up to 34.3°C, the minimum of $N(\Delta T)$ becomes more pronounced as seen in Fig. 4. A sequence of patterns representative of this parameter range is shown in Figs. 5(b)–5(f) for $T_t = 34.3$°C. Figure 5(b) ($\Delta T = 1.720$°C) corresponds to the roll region between $\Delta T_{c2}$ and $\Delta T_{c3}$. For Fig. 5(c) ($\Delta T = 5.425$°C), we have inverted hexagons, and no evidence of RB convection rolls is seen. For slightly larger $\Delta T$, however, an interesting pattern interaction occurs between the RB rolls which exist for large $\Delta T$ and the inverted hexagons which prevailed at smaller $\Delta T$. This interaction is similar to that seen in Figs. 3(b) and 3(c), which corresponds to $T_t < T^{ct1}$. The hexagons coexist and become aligned and commensurate with the rolls. This is shown in Figs. 5(d) and 5(e) which are for $\Delta T = 6.462$ and 7.249°C, respectively. The rolls are transverse in this case; the high-field limit for the purely nematic phase [13] seems no longer applicable. At even higher values of $\Delta T$, the RB rolls dominate, as seen in Fig. 5(f), which is for $\Delta T = 8.290$°C.

At even larger $T_t$ ($T_t = 34.4$ and 34.6°C in Fig. 4), the minimum of $N$ actually reaches the pure conduction state

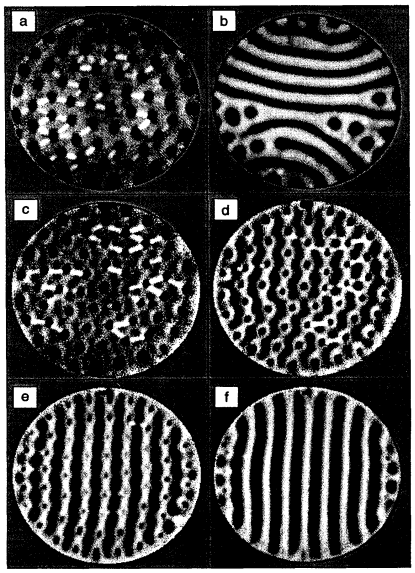


FIG. 5. Images of convection patterns. The magnetic field points from left to right. The values of $T_t$ and of $\Delta T$ in °C are (a) 34.0 and 5.281, (b) 34.3 and 1.720, (c) 34.3 and 5.425, (d) 34.3 and 6.462, (e) 34.3 and 7.249, and (f) 34.3 and 8.290.

$N=1$. Thus there is a second codimension-two point at $T_t=T^{c12}\simeq 34.35$°C. For larger $T_t$, the bifurcation points $\Delta T_{c4}$ where inverted-hexagon two-phase convection ceases are shown as crosses in Fig. 1. The onset of RB convection at $\Delta T_c^{RB}$ is given again as solid squares. Between these two bifurcations, we once more encounter a parameter range over which a layer of the isotropic fluid below the denser nematic layer is a stable state without convection. In this range of $T_t$, the RB pattern above $\Delta T_c^{RB}$ consists of transverse rolls without the admixture of black cells, similar to the pattern shown in Fig. 5(f).

Finally, we mention that ordinary RB convection was observed in our cell for $T_t > T_{NI}$ where the entire fluid layer is isotropic. One value of $\Delta T_c^{RB}$ is shown in Fig. 1 to the right of the vertical dashed line at $T_{NI}$. It falls on a smooth line through the $\Delta T_c^{RB}$ results in the two-phase region.

In the linear stability analysis, $\Delta T_{c1}$ and $\Delta T_{c4}$ are determined as a function of the interface position [3]. Although the interface is not held fixed in our experimental protocol, we can determine its position at the bifurcation point from the values of $T_t, T_b$, and $T_{NI}$ and from the conductivity of the two phases. The values which we obtained for $\Delta T_{c4}$ are larger than the theoretical result. We do not find this surprising since the theory neglects the interaction with the RB instability, and since it was evaluated only for simplifying assumptions which are not quantitatively applicable to our fluid. It is interesting to note that [1] $\Delta T_c^{RB}\sim d^{-3}$ and [3] $\Delta T_{c1,4}\sim d^3$. Thus, a small decrease of $d$ should separate the two instabilities.

We are grateful to H. Brand, F. Busse, P. C. Hohenberg, and L. Kramer for helpful discussions about the theoretical interpretation of our data. We thank S. Morris for his contributions to our understanding of nematic liquid crystals. This work was supported by the Department of Energy through Grant No. DE-FG03-87ER13738.

[a]Present address: Department of Physics, University of Oslo, P.O. Box 1048 Blindern, 0316 Oslo, Norway.

[1] H. Bénard, Rev. Gen. Sci. Pure Appl. **11**, 1261 (1900); **11**, 1309 (1900); Ann. Chim. Phys. **23**, 62 (1901); Lord Rayleigh, Philos. Mag. **32**, 529 (1916). For a recent review, see for instance F. Busse, in *Hydrodynamic Instabilities and the Transition to Turbulence*, edited by H. L. Swinney and J. P. Gollub (Springer, Berlin, 1981), p. 97.

[2] M. C. Cross and P. C. Hohenberg, Rev. Mod. Phys. (to be published).

[3] F. H. Busse and G. Schubert, J. Fluid Mech. **46**, 801 (1971).

[4] F. H. Busse, in *Mantle Convection, Plate Tectonics, and Global Dynamics*, edited by W. R. Peltier, The Fluid Mechanics of Astrophysics and Geophysics Vol. 4 (Gordon and Breach, New York, 1989), and references therein.

[5] For an interesting brief description of the current status of understanding of the mantle-convection problem, see R. A. Kerr, Science **258**, 1576 (1992).

[6] G. Schubert and J. M. Straus, J. Geophys. Res. **85**, 6505 (1980).

[7] Qualitative observations of hexagons and rolls in a nematic-isotropic two-phase system have been made by J. Salan and E. Guyon, J. Fluid Mech. **126**, 13 (1983) and by D. E. Fitzjarrald, J. Fluid Mech. **102**, 85 (1981).

[8] The Frederiks field is about 16 G. Thus the higher field is expected to be very effective in ordering otherwise multidomain samples. In the nematic phase, the convective onset is strongly field dependent. Thus the absence of a field dependence of the various bifurcation points reported here (other than $\Delta T_c^{RB}$) suggests that the anisotropy of the low-temperature (nematic) phase has little or no influence on the observed phenomena.

[9] J. Thoen, in *Phase Transitions in Liquid Crystals*, edited by S. Martellucci (Plenum, New York, 1992).

[10] D. A. Dunmur and W. H. Miller, J. Phys. (Paris), Colloq. **40**, C3-141 (1979).

[11] G. S. Iannacchione and D. Finotello, Phys. Rev. Lett. **69**, 2094 (1992).

[12] See, for instance, V. Steinberg, G. Ahlers, and D. S. Cannell, Phys. Scr. **32**, 534 (1985).

[13] Q. Feng, W. Pesch, and L. Kramer, Phys. Rev. A **45**, 7242 (1992).

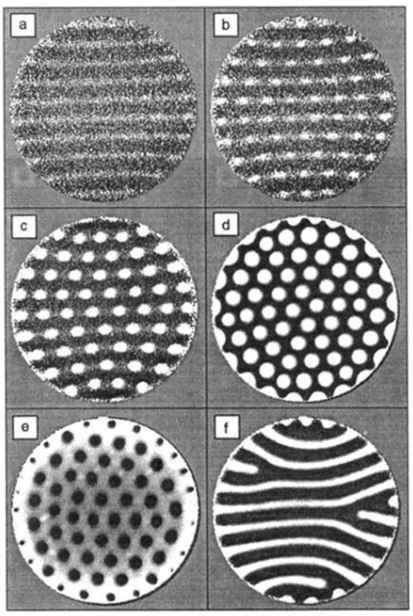


FIG. 3. Images of convection patterns. The magnetic field points from left to right. The values of $T_l$ and of $\Delta T$, in °C, are (a) 30.0 and 5.445, (b) 30.0 and 5.554, (c) 31.0 and 4.885, (d) 34.5 and 0.974, (e) 34.0 and 2.913, and (f) 31.0 and 5.592.

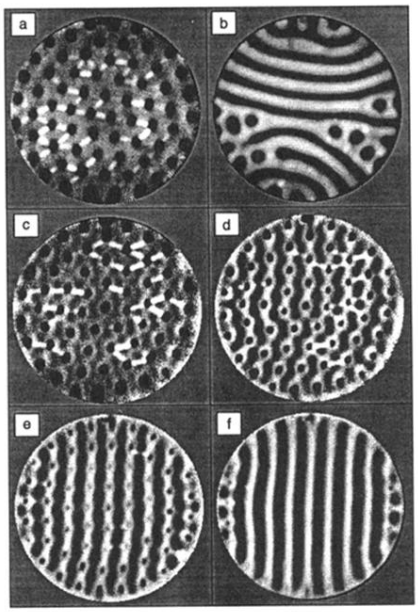


FIG. 5. Images of convection patterns. The magnetic field points from left to right. The values of $T_t$ and of $\Delta T$ in °C are (a) 34.0 and 5.281, (b) 34.3 and 1.720, (c) 34.3 and 5.425, (d) 34.3 and 6.462, (e) 34.3 and 7.249, and (f) 34.3 and 8.290.